Representation and Evolution of the Angular Momentum of the Light

P. Martelli and M. Martinelli, *Member, IEEE*

Dipartimento di Elettronica Informazione e Bioingegneria, Politecnico di Milano, 20133 Milano, Italy.

Manuscript received May 22, 2014; revised June 13, 2014; accepted June 18, 2014. Date of publication June 24, 2014; date of current version July 8, 2014. Corresponding author: P. Martelli (e-mail: paolo.martelli@polimi.it).

Abstract: A compact formalism for representing the angular momentum modes in paraxial optics is considered. The evolution of both spin and orbital components of angular momentum is described within such representation. A thorough analysis of the effect of reflection is carried out, and different kinds of reflective interfaces are analyzed. A general method for building the matrices representing the transformations of the spin and orbital angular momenta is introduced and applied to some meaningful examples concerning wave plates, mirrors, and prisms.

Index Terms: Orbital angular momentum, spin angular momentum, paraxial optics, optical communications.

1. Introduction

The awareness that free- and guided-wave optical modes can carry orbital angular momentum is opening new and interesting opportunities in optics and, in particular, optical communications [1]–[4]. As far as concern the propagation, the single-mode option, which dominated the optical transmission since the early 80s, contributed to the almost complete forgetfullness of the existence of a further quantum number held by the photon, the orbital angular momentum. This "fourth" label of the photon adds to the energy (or wavelength/frequency), the linear momentum (or the propagation wavevector) and the spin angular momentum (or polarization). The optical technology had since now deployed just the Wavelength Division Multiplexing (WDM) and more recently the Polarization Division Multiplexing (PDM), thanks to the development of practical coherent optical systems. In last years the orbital angular momentum has attracted a great research interest in view of Mode Division Multiplexing (MDM), which is envisaged as the technology enabling the next generation optical communication systems, in order to prevent the capacity crunch [5]. Moreover, the capability of manipulating the angular momentum is fundamental to implement not only effective mode multiplexers and demultiplexers for MDM, but also to realize network functionalities [6].

It is known from Allen *et al.* [7] that the Laguerre-Gauss beams carry on an orbital angular momentum, owing that the field possesses helical wavefronts, related to the azimuthal phase term $\exp(il\vartheta)$. Hence the phase pattern in a transverse plane rotates around the central beam axis and we can associate to this "twisted" light an orbital angular momentum vector **L**. We notice that these beams are also said optical vortices with topological charge l, corresponding to an orbital angular momentum of $l\hbar$ per photon. The Laguerre-Gauss beams also hold a state of

polarization, which can be represented as the sum of two orthogonal components. In particular, the right and left circular polarization states are classically described in a transverse plane by a rotating electric (magnetic) field vector. This rotation is associated to a spin angular momentum vector **S**. In the quantum picture a right/left circularly polarized beam carries an angular momentum of $\hbar$ per photon.

The full description of the angular momentum of the photons requires naturally the addition of orbital and spin parts. Quantum mechanics states that addition of angular momenta is possible only if the two addenda commute and whenever the spin is involved this is always verified. Thus the total angular momentum **J** of the photons belonging to one of the previous beams can be written as $\mathbf{J} = \mathbf{L} + \mathbf{S}$. Nevertheless the properties of the angular momentum are not identical for photons and electrons. The situation was synthesized by a seminal work of van Enk and Nienhuis in 1994 [8] and more recently further detailed by Barnett [9]. It was demonstrated that, in dealing with photons, the spin and orbital parts of the total angular momentum are observable physical quantities, but do not generate rotations and do not satisfy the quantum commutation rules of the angular momenta of matter particles (like electrons). Moreover, in paraxial optics it is possible to independently consider the orbital and spin components L_z and S_z, respectively, of the angular momentum along the propagation axis z. Indeed, the scalar field of the Laguerre–Gauss beams is a solution of the paraxial Helhmoltz equation. Other remarkable examples of paraxial beams are the higher-order Bessel beams with small transverse wave-vector [10] and the fiber-optic vortex modes [11] assuming the typical condition of weak guidance.

The aim of our present work is to give a contribution to the comprehension and manipulation of the angular momentum of the light by introducing a compact and effective matrix notation for both spin and orbital angular momenta. We will exploit this notation to study the evolution of the total angular momentum.

2. Angular momentum representation

The operator associated to S_z can be represented by a 2×2 diagonal matrix in the two-dimension Hilbert space of the polarization states, by choosing the circular states as orthogonal basis. In fact, the right/left circular states of polarization are eigenstates of the photon spin angular momentum with eigenvalues ± 1, in $\hbar$ unit, obtaining the diagonal matrix

$$S_z = \begin{bmatrix} 1 & 0 \\ 0 & -1 \end{bmatrix}. \tag{1}$$

Regarding the operator associated to L_z, we should consider the infinite-dimension Hilbert space having as orthogonal basis the eigenstates of the orbital angular momentum with integer eigenvalues, in $\hbar$ unit. Indeed, we choose to represent L_z in the two-dimension subspace generated by the eigenstates with eigenvalues $\pm l$, because in this work we focus onto optical transformations that couple modes with same absolute value of L_z and opposite handedness. According to this choice, the matrix representation is

$$L_z = \begin{bmatrix} l & 0 \\ 0 & -l \end{bmatrix}. \tag{2}$$

In order to represent the total angular momentum operator, we have to sum the proper extensions in a 4-dimension Hilbert space of the 2×2 matrices representing L_z and S_z. The mathematical operation that carries out this extension is the Kronecker product (or direct product) [12] by the identity operator I. We choose to left-multiply L_z by I and right-multiply S_z by I, to build the total angular momentum operator

$$J_z = L_z \otimes \mathrm{I} + \mathrm{I} \otimes S_z. \tag{3}$$

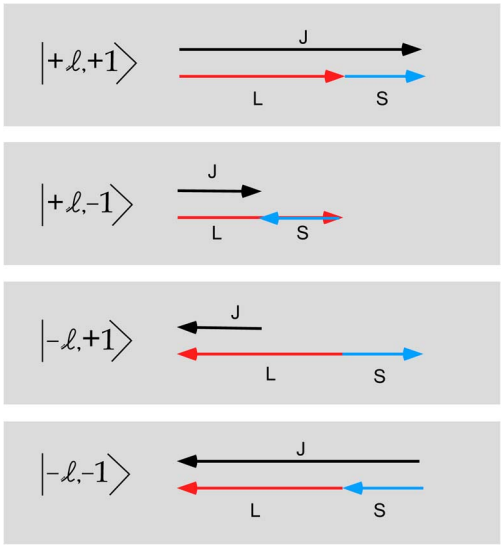

Fig. 1. Vectorial picture of the total angular momentum modes. The total angular momentum **J** is the sum of the spin angular momentum **S** and the orbital angular momentum **L**. The vectors are represented along the direction of the propagation axis.

Considering the above introduced 2×2 matrices for L_z and S_z, we obtain, substituting (1) and (2) in (3), the following 4×4 matrix representing the total angular momentum

$$J_z = \begin{bmatrix} l+1 & 0 & 0 & 0 \\ 0 & l-1 & 0 & 0 \\ 0 & 0 & -l+1 & 0 \\ 0 & 0 & 0 & -l-1 \end{bmatrix}. \tag{4}$$

Such a matrix is diagonal, hence the total angular momentum eigenstates (or modes) are the basis of this representation and can be identified through the compact notation $|\pm l, \pm 1\rangle$, satisfying the eigenvalue equation

$$J_z|\pm l, \pm 1\rangle = (\pm l, \pm 1)|\pm l, \pm 1\rangle. \tag{5}$$

In Fig. 1 a vectorial picture of such four modes is given. We remark that this representation is based on a complete description of the total angular momentum modes as combination of mutually independent orbital and spin angular momentum modes, according to Refs. [13], [14].

Once determined a representation of the total angular momentum modes, it is interesting to evaluate the evolution of such modes under the perturbations occurring during the propagation. Hereafter, we will consider a generic case of perturbation acting on both orbital and spin angular momenta. We can build the representative matrix in the 4-dimension Hilbert space of the total angular momentum, starting from the 2×2 matrices $M^{(2,\text{orbital})}$ and $M^{(2,\text{spin})}$ related to the orbital and spin angular momentum sub-spaces, respectively, in the following way:

$$M^{(4)} = \left(M^{(2,\text{orbital})} \otimes \mathrm{I}\right) \cdot \left(\mathrm{I} \otimes M^{(2,\text{spin})}\right). \tag{6}$$

We remark that $M^{(2,\text{spin})}$ is given by the Jones matrix in the circular polarization basis. Eq. (6) indicates that the 4×4 matrix representing a transformation of the total angular momentum is given by the product of the two 4×4 matrices extending the 2×2 matrices for the orbital and spin part, through the Kronecker product by the identity matrix in the order expressed by (3). Moreover, the choice of the order of the factors in the matrix multiplication of (6) is indifferent,

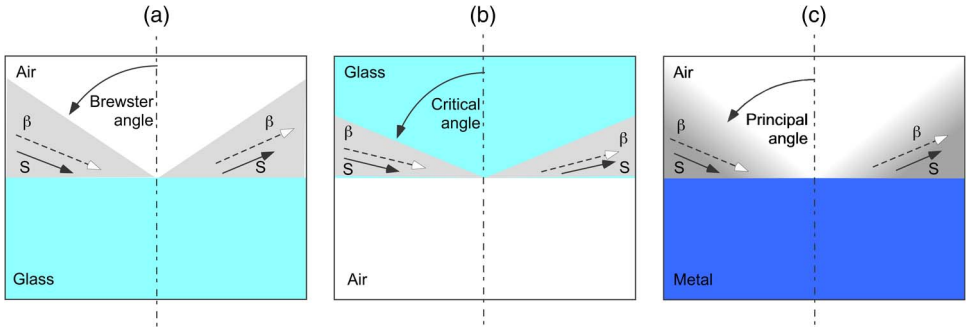

Fig. 2. Three typical mirror interfaces. (a) From a lower-index to higher-index dielectric; (b) from higher-index to lower-index dielectric; (c) from dielectric to conductor (like a metal). In gray, the range of angles for which the handedness of the photon spin (with respect to the propagation direction) is maintained. For the complementary angles, the handedness is reversed. The transition is sharp in the dielectric interface and smooth in the metal interface.

because the two factors refer to the orthogonal sub-spaces of orbital and spin parts, respectively, and we can equivalently write

$$M^{(4)} = \left(\mathrm{I} \otimes M^{(2,\mathrm{spin})}\right) \cdot \left(M^{(2,\mathrm{orbital})} \otimes \mathrm{I}\right). \tag{7}$$

3. Effect of the reflection on spin and orbital angular momenta

In the present section, we report some general considerations about the reflection, detailing the interaction of the two parts of the angular momentum with reflective surfaces and the effect of this interaction on the angular momentum handedness. Before proceeding, it is important to distinguish between two kinds of beam incidence: the front incidence and the skewed incidence. In terms of the angle between the beam and the normal to the mirror surface, the above cases correspond to the low-angle incidence or high-angle incidence. For the spin component of the total angular momentum the situation must be further specified as function of the kind of interface that originated the mirror effect. Three types of interfaces summarize the main situations: a) from lower-index to higher-index dielectric; b) from higher-index to lower-index dielectric; c) from dielectric to conductor (like a metal). Following Clarke and Grainger [15], the analysis of the interaction can be synthesized saying that in all the three situations there is a specific angle of incidence with respect to the direction normal to the interface: the Brewster angle in a), the critical angle in b), the principal angle in c), which separates the angular range of incidence into two regions. Below the above-specified angles the spin reverses its handedness, as shown in Fig. 2, otherwise the spin maintains its handedness. Referring to Fig. 2, in both cases a) and b) the transition effect between the two different regions is rather sharp, while in case c), where the reflection occurs by a metallic mirror, the effect is smooth.

On the other hand, the behaviour after reflection of the orbital angular momentum, which is a global property of the whole beam related to the azimuthal phase term, is quite different from the spin, which is a local property [16]. Indeed, the photons of a single beam, i.e., characterized by a single wavefront, must have the same orbital angular momentum, while they can have different values of spin angular momentum, according to the different positions in the wavefront. The effect of the mirror is to exchange right and left, that is to make the coordinate change $x \to -x$ in the reflected reference frame, equivalent to the azimuth transformation $\vartheta \to \pi - \vartheta$. Apart a phase shift of $l\pi$, the effect of the reflection by a mirror onto an eigenstate of the orbital angular momentum with eigenvalue l is equivalent to the sign inversion $l \to -l$. Hence, whatever be the type of reflection considered, either front or skewed, the handedness of the orbital angular momentum is always reversed.

The above analysis points out that the reflection by a mirror can operate differently on the two parts of the photon total angular momentum, depending on the specific kind of reflection.

4. Examples of angular momentum transformation

Hereafter, we will apply the introduced formalism for describing the transformation of the angular momentum of a beam propagating through one of the following remarkable examples of optical elements:

i) a birefringent retarder plate, which acts only on the spin angular momentum;
ii) a Dove prism exploiting total internal reflection, which acts only on the orbital angular momentum;
iii) a mirror, which acts on both spin and orbital angular momenta.

4.1. Birefringent retarder plate

As far as concern the perturbation given by the birefringence, it uniformly affects the direction of the vector field and hence it acts only on the spin component of the total angular momentum, which is related to the state of polarization, keeping the orbital angular momentum unaltered. It is customary to analyze the perturbations acting on the spin angular momentum of the beam by means of the Jones formalism developed for the polarization of the light. Since the circular states of polarization are the eigenstates of the spin angular momentum, we choose such states as basis for the representation of the Jones matrices. The relation between a generic Jones matrix $M^{(\mathrm{H-V})}$ in the usual representation of the H–V basis, constituted by the horizontal and vertical linear states of polarization, and the corresponding Jones matrix $M^{(\mathrm{circ})}$ in the circular basis, according to [17], is given by

$$M^{(\mathrm{circ})} = \begin{bmatrix} a_{11} & a_{12} \\ a_{21} & a_{22} \end{bmatrix} = \frac{1}{2}\begin{bmatrix} b_{11}+b_{22}-i(b_{12}-b_{21}) & b_{11}-b_{22}+i(b_{12}+b_{21}) \\ b_{11}-b_{22}-i(b_{12}+b_{21}) & b_{11}+b_{22}+i(b_{12}-b_{21}) \end{bmatrix} \tag{8}$$

where

$$M^{(\mathrm{H-V})} = \begin{bmatrix} b_{11} & b_{12} \\ b_{21} & b_{22} \end{bmatrix}. \tag{9}$$

Once obtained the Jones matrix in the proper representation, we have to extend it as operator in the 4-D Hilbert space. In the hypothesis that the birefringence be homogeneous in the whole cross section of the propagating beam, only the spin part will be affected by the Jones operation and, as a consequence, we apply to (8) the Kronecker product, as made for the spin part of the total angular momentum in the second term of the left side of (6). Hence, we obtain the following extended 4×4 matrix

$$M^{(4)} = \mathrm{I} \otimes M^{(\mathrm{circ})} = \begin{bmatrix} 1 & 0 \\ 0 & 1 \end{bmatrix} \otimes \begin{bmatrix} a_{11} & a_{12} \\ a_{21} & a_{22} \end{bmatrix} = \begin{bmatrix} a_{11} & a_{12} & 0 & 0 \\ a_{21} & a_{22} & 0 & 0 \\ 0 & 0 & a_{11} & a_{12} \\ 0 & 0 & a_{21} & a_{22} \end{bmatrix}. \tag{10}$$

For instance, we can consider a half-wave plate, which is represented by the standard Jones matrix in H–V basis

$$M^{(\mathrm{H-V})} = \begin{bmatrix} 1 & 0 \\ 0 & -1 \end{bmatrix}. \tag{11}$$

Taking into account (8)–(11), we obtain the following 4×4 matrix for the half-wave plate

$$M^{(\mathrm{circ})}_{\mathrm{hwp}} = \begin{bmatrix} 1 & 0 \\ 0 & 1 \end{bmatrix} \otimes \begin{bmatrix} 0 & 1 \\ 1 & 0 \end{bmatrix} = \begin{bmatrix} 0 & 1 & 0 & 0 \\ 1 & 0 & 0 & 0 \\ 0 & 0 & 0 & 1 \\ 0 & 0 & 1 & 0 \end{bmatrix}. \tag{12}$$

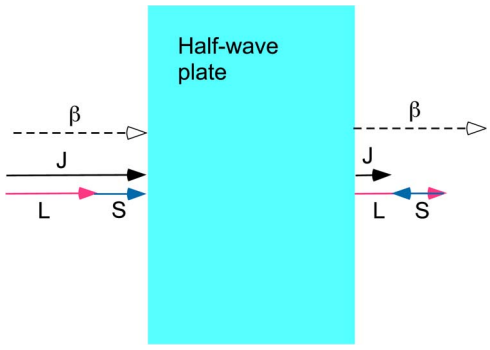

Fig. 3. A beam passing through a half-wave plate, where only the spin angular momentum **S** is reversed with respect to the propagation direction.

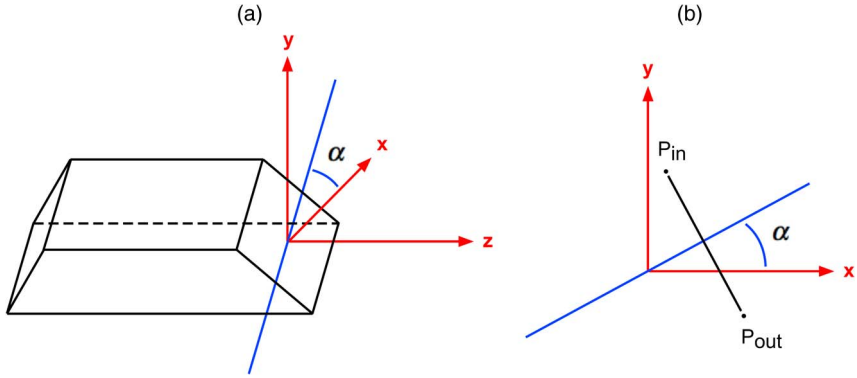

Fig. 4. (a) Sketch of a Dove prism with the totally reflective face rotated by an angle α with respect to the horizontal plane *xz*. (b) Representation of the action of the rotated Dove prism, which transforms an input image point P_{in} into an output image point P_{out} through an inversion around a plane parallel to the totally reflective prism face, whose section on the transverse plane *xy* is depicted by the blue line.

The application of this matrix to the basis vectors, which are the eigenvectors of the diagonal matrix (4) representing the total angular momentum, transforms the eigenstates $|\pm l, \pm 1\rangle$ into $|\pm l, \mp 1\rangle$. The above result confirms that a half-wave plate, introducing a homogeneous perturbation in the transverse plane, does not change the orbital angular momentum value, but changes only the spin angular momentum value, which is inverted, as also shown by Fig. 3.

4.2. Dove prism

The most popular example of optical element inducing a perturbation acting only on the orbital part of the total angular momentum is given by the Dove prism, which works by means of a total internal reflection between two refractions of the beam crossing it. The optical beam at the exit of the prism returns in the same direction of the entrance, while the image is inverted with respect to a plane parallel to the prism face involved in the total internal reflection. Considering such inversion plane as the horizontal plane *xz*, it results that the azimuth of the points of an image is reversed, i.e. the Dove prism operates the transformation $\vartheta \rightarrow -\vartheta$. Moreover, if the face of total internal reflection is rotated of an angle α around the propagation axis *z*, then the image is rotated [18] by the double angle 2α after the inversion, i.e., $\vartheta \rightarrow 2\alpha - \vartheta$, as shown in Fig. 4. Hence the Dove prism transforms the azimuthal phase term associated to an orbital angular momentum eigenstate with eigenvalue *l* in the following way: $\exp(il\vartheta) \rightarrow \exp(il2\alpha) \cdot \exp(-il\vartheta)$. This means that a beam carrying an orbital angular momentum reverses its handedness and

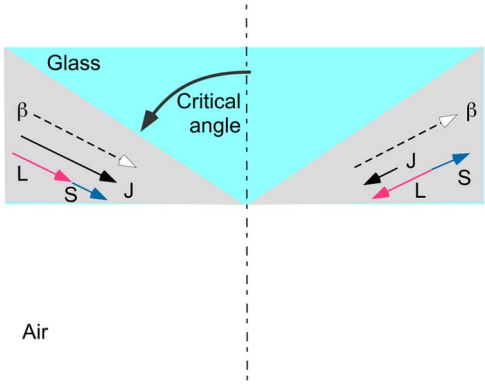

Fig. 5. A beam hitting a prism in total internal reflection, where only the orbital angular momentum **L** is reversed with respect to the propagation direction.

acquires a phase shift $l2\alpha$ after a Dove prism. It is worthwhile to remark that this dependence of the phase shift on both the angle of rotation of the Dove prism and the orbital angular momentum value at the entrance allows for exploiting interferometric schemes based on rotated Dove prisms for demultiplexing beams with different values of orbital angular momentum [19]–[21].

More in detail, considering a balanced Mach–Zehnder interferometer with two Dove prisms mutually rotated of an angle α in the two respective arms, it is possible to separate two different orbital angular momentum modes with $2\alpha\Delta l$ equal to an odd multiple of π, at the two output ports of the interferometer. For instance, we can discriminate modes with $\Delta l = \pm 1, \pm 3, \ldots$ by $\alpha = \pi/2$, modes with $\Delta l = \pm 2, \pm 6, \ldots$ by $\alpha = \pi/4$, and so on. In general, it is possible to separate any finite set of different orbital angular momentum modes by means of a binary tree of Mach–Zehnder interferometers with properly oriented Dove prisms in the arms. This all-optical technique of mode demultiplexing is very promising in view of MDM data communications systems, where independent channels corresponding to different orbital angular momentum modes are transmitted, because it avoids the use of complex and power-consuming ultra-high-speed digital-signal-processing electronics for correctly detecting each mode.

According to our formalism, the action of a rotated Dove prism is represented, in the 2-D subspace generated by the orbital angular momentum eigenstates of eigenvalues $\pm l$, by the matrix

$$M^{(2)}_{\text{Dove}} = \begin{bmatrix} 0 & \exp(-il2\alpha) \\ \exp(il2\alpha) & 0 \end{bmatrix} \tag{13}$$

which is anti-symmetric, owing to the change of the orbital angular momentum handedness. On the other hand the spin angular momentum handedness is conserved, as reported by [22]. We can explain this behavior, as shown by Fig. 5, by noticing that the total internal reflection occurring in the Dove prism acts differently on the spin and orbital parts of the angular momentum. The spin angular momentum handedness is maintained because the incidence angle is greater than the critical angle in the total internal reflection (as shown in Fig. 2(b)), while the orbital angular momentum handedness is reversed because the reflection inverts the image. In order to extend the representation of the rotated Dove prism into the proper 4-dimension Hilbert space of the total angular momentum, taking into account that only the orbital part is affected, we simply have to carry out a left Kronecker product of the 2×2 matrix in (13) by the identity matrix. Hence, we obtain the 4×4 matrix

$$M^{(4)}_{\text{Dove}} = M^{(2)}_{\text{Dove}} \otimes \mathsf{I} = \begin{bmatrix} 0 & 0 & \exp(-il2\alpha) & 0 \\ 0 & 0 & 0 & \exp(-il2\alpha) \\ \exp(il2\alpha) & 0 & 0 & 0 \\ 0 & \exp(il2\alpha) & 0 & 0 \end{bmatrix}. \tag{14}$$

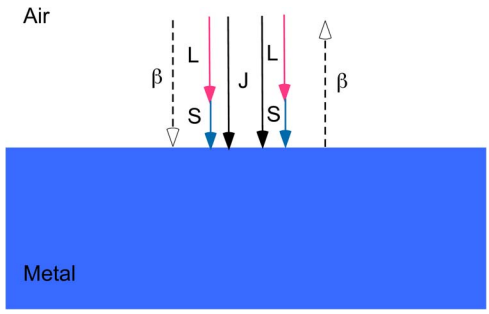

Fig. 6. A beam hitting a front mirror, which reverses both spin and orbital parts of the total angular momentum **J** with respect to the propagation direction.

4.3. Front mirror

A very meaningful example of transformation of the total angular momentum, perturbing both spin and orbital angular momenta, is the reflection by a mirror in case of normal incidence. According to the analysis reported in Section 3, the 2 × 2 matrix representing the action of a front mirror on the orbital angular momentum is

$$M_{\text{mirror}}^{(2,\text{orbital})} = \exp(il\pi)\begin{bmatrix} 0 & 1 \\ 1 & 0 \end{bmatrix} = (-1)^l \begin{bmatrix} 0 & 1 \\ 1 & 0 \end{bmatrix} \tag{15}$$

owing to the fact that the left-right inversion due to the mirror changes the sign of the orbital angular momentum and shifts the phase of $l\pi$. As concerns the spin angular momentum, the action of the front mirror is to transform a right (left) circular state of polarization into a left (right) circular state, accompanied by a phase shift of π giving the nodality of the field onto the metallic mirror (i.e., the incident and the reflected fields cancel out at the metal surface). Hence, the 2 × 2 matrix representing a front metallic mirror in the spin angular momentum subspace is

$$M_{\text{mirror}}^{(2,\text{spin})} = \exp(i\pi)\begin{bmatrix} 0 & 1 \\ 1 & 0 \end{bmatrix} = -\begin{bmatrix} 0 & 1 \\ 1 & 0 \end{bmatrix}. \tag{16}$$

Using the general recipe introduced in Section 2, we can substitute (15) and (16) into (6) for obtaining the following 4 × 4 matrix:

$$M_{\text{mirror}}^{(4)} = \left(M_{\text{mirror}}^{(2,\text{orbital})} \otimes \mathrm{I}\right) \cdot \left(\mathrm{I} \otimes M_{\text{mirror}}^{(2,\text{spin})}\right) = (-1)^{l+1} \begin{bmatrix} 0 & 0 & 0 & 1 \\ 0 & 0 & 1 & 0 \\ 0 & 1 & 0 & 0 \\ 1 & 0 & 0 & 0 \end{bmatrix}. \tag{17}$$

This matrix is anti-diagonal, since the normal reflection by a mirror reverses the handedness of both orbital and spin angular momenta, according to the analysis reported in the previous section. We also have experimented this handedness change, converting a linearly polarized Gaussian He–Ne laser beam into a circularly polarized doughnut beam, through a quarter wave-plate and a spiral phase-plate, and analyzing it after reflection. In Fig. 6 a pictorial view of the behavior of the propagation wave vector, represented by a dashed arrow, and of the angular momentum vectors **L**, **S**, **J** is shown. It is evident that the propagation direction of the light is reversed, while the direction **L**, **S**, **J** is not changed. This is in agreement to the fact that the handedness of angular momenta changes the sign, which depends on the orientation of **L**, **S**, **J** with respect to the propagation direction. Therefore, we can say that the physical action of normal reflection by a metallic mirror is equivalent to the inversion of *z*-axis of a cartesian reference frame. Indeed, such a reference mirroring inverts the *z*-component of usual vectors (like position, linear momentum, and, hence wave vector of light), also called polar vectors, while it does

not invert the *z*-component of angular momentum vectors (like mechanical torque and angular momenta of light), also called axial vectors or pseudo-vectors [23], [24].

5. Conclusion

The results obtained in the previous sections set the basis for the representation of the total angular momentum modes in paraxial optics. The analysis takes into account that the different nature of the spin and orbital parts of the light angular momentum impacts on the evolution of the total angular momentum.

In this work we propose a general method for describing the evolution of the total angular momentum, in case of typical optical components within the validity of paraxial optics, comprising lenses, wave-plates, prisms and mirrors. In particular a thorough analysis of the effect of the reflection onto spin and orbital angular momenta is presented.

References

[1] I. B. Djordjevic, "Heterogeneous transparent optical networking based on coded OAM modulation," *IEEE Photon. J.*, vol. 3, no. 3, pp. 531–537, Jun. 2011.

[2] P. Martelli, A. Gatto, P. Boffi, and M. Martinelli, "Free-space optical transmission with orbital angular momentum division multiplexing," *Electron. Lett.*, vol. 47, no. 17, pp. 972–973, Aug. 2011.

[3] J. Wang *et al.*, "Terabit free-space data transmission employing orbital angular momentum multiplexing," *Nat. Photon.*, vol. 6, no. 7, pp. 488–496, Jul. 2012.

[4] D. Bozinovic *et al.*, "Terabit-scale orbital angular momentum mode division multiplexing in fibers," *Science*, vol. 340, no. 6140, pp. 1545–1548, Jun. 2013.

[5] A. R. Chraplyvy, "The coming capacity crunch," in *Proc. Eur. Conf. Opt. Commun.*, 2009, pp. 1.

[6] J. Wang and A. Willner, "Using orbital angular momentum modes for optical transmission," presented at the Opt. Fiber Commun. Conf., San Francisco, CA, USA, 2014, Paper W4J.5.

[7] L. Allen, M. W. Beijersbergen, R. J. C. Spreeuw, and J. P. Woerdman, "Orbital angular momentum of light and the transformation of Laguerre–Gaussian laser modes," *Phys. Rev. A, At. Mol. Opt. Phys.*, vol. 45, no. 11, pp. 8185–8189, Jun. 1992.

[8] S. J. Van Enk and G. Nienhuis, "Spin and orbital angular momentum of photons," *Europhys. Lett.*, vol. 25, no. 7, pp. 497–501, Mar. 1994.

[9] S. M. Barnett, "Rotation of electromagnetic fields and the nature of optical angular momentum," *J. Mod. Opt.*, vol. 57, no. 14/15, pp. 1339–1343, Aug. 2010.

[10] P. Martelli, M. Tacca, A. Gatto, G. Moneta, and M. Martinelli, "Gouy phase shift in nondiffracting Bessel beams," *Opt. Exp.*, vol. 18, no. 7, pp. 7108–7120, Mar. 2010.

[11] K. N. Alexeyev, T. A. Fadeyeva, A. V. Volyar, and M. S. Soskin, "Optical vortices and the flow of their angular momentum in a multimode fibre," *Semicond. Phys. Quantum Electron. Optoelectron.*, vol. 1, no. 1, pp. 82–89, 1998.

[12] H. Ľtkepohl, *Handbook of Matrices*. New York, NY, USA: Wiley, 1996.

[13] I. B. Djordjevic, "Multidimensional QKD based on combined orbital and spin angular momenta of photon," *IEEE Photon. J.*, vol. 5, no. 6, p. 7600112, Dec. 2013.

[14] V. D'Ambrosio *et al.*, "Complete experimental toolbox for alignment-free quantum communication," *Nat. Commun.*, vol. 3, 7, p. 961, Jul. 2012.

[15] D. Clarke and J. F. Grainger, *Polarized Light and Optical Measurement*. Oxford, U.K.: Pergamon, 1971.

[16] L. Allen and M. Padgett, "Equivalent geometric transformations for spin and orbital angular momentum of light," *J. Mod. Opt.*, vol. 54, no. 4, pp. 487–491, Mar. 2007.

[17] C. Brosseau, *Fundamentals of Polarized Light*. New York, NY, USA: Wiley, 1998.

[18] R. H. Ginsberg, "Image rotation," *Appl. Opt.*, vol. 33, no. 34, pp. 8105–8108, Dec. 1994.

[19] J. Leach, M. J. Padgett, S. M. Barnett, S. Franke-Arnold, and J. Courtial, "Measuring the orbital momentum of a single photon," *Phys. Rev. Lett.*, vol. 88, no. 25, pp. 257901-1–257901-4, Jun. 2002.

[20] J. Leach *et al.*, "Interferometric methods to measure orbital and spin or the total angular momentum of a single photon," *Phys. Rev. Lett.*, vol. 92, no. 1, pp. 013601-1–013601-4, Jan. 2004.

[21] P. Boffi, P. Martelli, A. Gatto, and M. Martinelli, "Mode-division multiplexing in fibre-optic communications based on orbital angular momentum," *J. Opt.*, vol. 15, 7, pp. 075403, Jul. 2013.

[22] J. M. Padgett and J. P. Lesso, "Dove prisms and polarized light," *J. Mod. Opt.*, vol. 46, no. 2, pp. 175–179, Feb. 1999.

[23] S. L. Altmann, *Icons and Symmetries*. Oxford, U.K.: Clarendon, 1992.

[24] G. B. Arfken and H. J. Weber, *Mathematical Methods for Physicists*, 5th ed. San Diego, CA, USA: Academic, 2001.